

## Polarization properties of dielectronic satellite lines in the K-shell x-ray spectra of B-like Fe XXII

A S Shlyaptseva<sup>†</sup>, R C Mancini<sup>†</sup>, P Neill<sup>†</sup> and P Beiersdorfer<sup>‡</sup>

<sup>†</sup> Department of Physics, University of Nevada, Reno, NV 89557-005, USA

<sup>‡</sup> Lawrence Livermore National Laboratory, Livermore, CA 94550, USA

Received 23 October 1998

**Abstract.** We report the results of a combined theoretical and experimental study of B-like dielectronic recombination satellite lines excited by an electron beam. Polarization sensitive spectra were accumulated at the Lawrence Livermore electron beam ion trap facility. Three beam energies were chosen in the region of maximum B-like Fe satellite emission. At each energy, spectra were obtained using two LiF crystals of differing polarization sensitivities. Polarization-dependent spectra have been calculated using the degree of polarization of single lines computed with a photon density matrix formalism. The agreement between the experiment and theory is very good. Two spectral features were observed to have polarizations that were particularly sensitive to the electron beam energy. Spectral features with this property are candidates as diagnostics of energy and direction of electron beams in plasmas.

### 1. Introduction

The degree of linear polarization of x-ray lines from highly charged ions can provide information on the anisotropy of the electron distribution function in high-temperature plasmas. In particular, the polarization of x-ray lines can be used as a spectroscopy diagnostic for the energy and directionality of electron beams in astrophysical and laboratory plasmas [1–5]. The understanding of polarized line emission from high-temperature plasmas requires modelling of different excitation mechanisms of line transitions that can lead to alignment of energy levels, such as direct electron-impact excitation, cascade contributions, and dielectronic recombination. The construction of reliable models requires that each component be tested against experimental benchmarks. The aim of this paper is to calculate the polarization of K-shell lines produced by dielectronic recombination and test these results against laboratory data produced under well controlled conditions. These fundamental studies are important for the development of plasma diagnostics using polarization spectroscopy.

The electron beam ion trap (EBIT) is a powerful tool capable of creating very highly charged ions for atomic structure, electron–ion collision and other spectroscopic studies [6]. Furthermore, EBIT offers an excellent opportunity to observe polarization effects in x-ray line emission in experiments performed under well controlled conditions. In turn, these measurements can be used to make detailed comparisons with theoretical calculations before applying them to the analysis of polarized spectra from complicated systems like plasmas. Recently, polarization measurements of x-ray lines of He- and Li-like Fe ions excited by electron impact were performed by Beiersdorfer *et al* [7, 8] at the Livermore EBIT. We have published the results on the analysis of polarization-dependent spectra of dielectronic satellite lines of Li- and Be-like Fe ions produced at the Livermore EBIT elsewhere [9, 10]. In this paper,

we develop and extend our previous studies and present an extensive analysis of polarization-dependent spectra of dielectronic satellite lines of B-like Fe. Theoretical and experimental results of the polarization properties of spectral features formed by the overlapping and blending of dielectronic satellite lines are discussed in detail. Our calculated polarization-dependent spectra are compared with experimental spectra observed at the Livermore EBIT. To this end, dielectronic satellite spectra were simultaneously recorded with two crystal spectrometers, which acted as polarization analysers by reflecting polarization states associated with directions parallel and perpendicular to the electron beam axis with different efficiencies. The dielectronic satellite spectrum is significantly polarized and, in general, the two polarization-dependent spectra have different intensity distributions. The details of these spectra also depend strongly on the energy of the electron beam. In section 2 we develop our theoretical approach for the calculation of polarization-dependent spectra of dielectronic satellite lines. Specifically, in section 2.1 we briefly discuss the basic formalism presented in detail in our previous paper [10], in section 2.2 we discuss the results of the calculations of atomic and polarization characteristics, and in section 2.3 we display theoretical, polarization-dependent spectra. Experimental details and measurements are given in section 3. In section 4 we discuss the experimental and theoretical results, and their comparison. Finally, in section 5 we present our conclusions.

## 2. Theoretical approach

### 2.1. Formalism

A detailed discussion of the theoretical formalism used for the calculation of the polarization-dependent spectra is presented in [10]. Here, we mention only the main points. The degree of polarization of line transitions excited by an electron beam observed in a direction perpendicular to the electron beam is defined as:

$$P_0 = \frac{I_{\parallel} - I_{\perp}}{I_{\parallel} + I_{\perp}} \quad (1)$$

where  $I_{\parallel}$ ,  $I_{\perp}$  are the photon intensities associated with electric vectors polarized parallel and perpendicular to the electron beam, respectively. If  $\theta$  is the angle between the axis of the electron beam and the direction of observation, the total intensity observed at  $\theta = 90^\circ$  is  $I(90^\circ) = I_{\parallel} + I_{\perp}$ .

The intensities of dielectronic satellite lines associated with different polarization states have the following form:

$$I_{\parallel}(s) = \frac{3}{2} Q_d(s) \exp(-((E_b - E_a(s))/\Delta E)^2) \frac{1 + P_0}{3 - P_0} \quad (2)$$

$$I_{\perp}(s) = \frac{3}{2} Q_d(s) \exp(-((E_b - E_a(s))/\Delta E)^2) \frac{1 - P_0}{3 - P_0} \quad (3)$$

here  $Q_d(s)$  is the intensity factor, and  $E_a(s)$  is the auto-ionization energy. In equations (2) and (3), the beam of electrons is characterized by a Gaussian distribution function centred at the beam energy  $E_b$  with a width  $\Delta E$ . Thus, to calculate the intensity of a dielectronic satellite line  $s$  associated with parallel and perpendicular polarization states, we need to know the atomic characteristics,  $Q_d(s)$  and  $E_a(s)$ , and the degree of polarization of each satellite line  $P_0(s)$ .

To describe the polarization properties of dielectronic satellite line emission we use a photon density matrix formalism. We consider the representation of the total momentum of the system. The target ion in the initial state (before recombination) and an incident electron is the initial state of the system characterized by the index  $i$ . The target ion in the auto-ionization

**Table 1.** Atomic and polarization characteristics for dielectronic satellite transitions  $1s^22s^22p^2 \rightarrow 1s^22s^22p$  of B-like Fe.  $\lambda$  are wavelengths,  $A_r$  are radiative probabilities,  $Q_d$  are intensity factors,  $E_a$  are auto-ionization energies, and  $P_0$  are the values of maximum degree of polarization of transitions. Number in square brackets denote powers of 10.

Peak	Line	[16]	Transition	$J_a - J_f$	$\lambda(\text{\AA})$	$A_r(s^{-1})$	$Q_d(s^{-1})$	$E_a(eV)$	$P_0$
3	1	B2	$^2S - ^2P$	$\frac{1}{2} - \frac{3}{2}$	1.8795	2.88[+14]	5.68[+13]	4809.1	0.0
	2	B3	$^2P - ^2P$	$\frac{3}{2} - \frac{3}{2}$	1.8814	5.77[+14]	1.21[+14]	4802.5	-0.75
1	3	B5	$^2D - ^2P$	$\frac{3}{2} - \frac{1}{2}$	1.8821	3.07[+14]	2.51[+14]	4785.4	0.6
	4	B4	$^2P - ^2P$	$\frac{1}{2} - \frac{1}{2}$	1.8822	5.20[+14]	9.03[+12]	4785.1	0.0
2	5	B6	$^2D - ^2P$	$\frac{5}{2} - \frac{3}{2}$	1.8849	2.05[+14]	3.34[+14]	4790.4	0.5
	6	B8	$^2D - ^2P$	$\frac{3}{2} - \frac{3}{2}$	1.8863	3.80[+13]	3.12[+13]	4785.4	-0.75
	7	B9	$^4P - ^2P$	$\frac{5}{2} - \frac{3}{2}$	1.8916	2.89[+13]	1.31[+13]	4766.9	0.5

state is characterized by the index  $a$ . The target ion in the final state (after recombination and emission of the photon) and the emitted photon is the final state of the system characterized by the index  $f$ . The quantization axis  $z$  is taken along the direction of the electron beam. We assume that the auto-ionizing states in the B-like ions are populated by electron capture originating only in the ground state  $1s^22s^2\ ^1S_0$  of Be-like ions. This approximation is reasonable considering that we will compare theoretical results with experimental data recorded at the Livermore EBIT where it can be safely assumed, under the experimental conditions, that the largest population of Be-like ions is concentrated in the ground state.

We have shown how the elements of photon density matrix are connected with the degree of polarization (see equations (22)–(28) of [10]). Finally, we got the expression for the degree of polarization in the following simple form (see equation (29) in [10]):

$$P(s) = -\frac{3 \sin^2 \theta B_2(s)}{2\sqrt{10}B_0(s) + (3 \cos^2 \theta - 1)B_2(s)} \quad (4)$$

here  $B_L(s)$  is the so-called polarization moment of the ion:

$$B_L(s) = (-1)^{1-J_f-S_a} (2L+1) \begin{pmatrix} l & L & l \\ 0 & 0 & 0 \end{pmatrix} \begin{Bmatrix} L_a & L & L_a \\ J_a & S_a & J_a \end{Bmatrix} \begin{Bmatrix} J_a & L & J_a \\ j_{ph} & J_f & j_{ph} \end{Bmatrix} \quad (5)$$

where  $\begin{pmatrix} \end{pmatrix}$  are the 3- $j$  symbols, and  $\begin{Bmatrix} \end{Bmatrix}$  are the 6- $j$  symbols. In our case, where only electric dipole transitions contribute to the dielectronic satellite emission,  $L$  can be equal to 0 or 2. If  $B_2(s) = 0$ , then the line has a zero degree of polarization. For nonzero  $B_2(s)$ , the degree of polarization  $P(s)$  is nonzero and has a maximum value for  $\theta = 90^\circ$ . The results of the calculation of  $P_0(s)$  are discussed in the next section.

## 2.2. Atomic and polarization characteristics

In table 1 the atomic characteristics, namely wavelengths  $\lambda$ , radiative transition probabilities  $A_r$ , intensity factors  $Q_d$ , and auto-ionization energies  $E_a$ , used to calculate polarization-dependent spectra of B-like Fe dielectronic satellite line spectra are listed. Also displayed in table 1 is the degree of polarization of each dielectronic satellite line  $P_0(s)$ , which has been computed using the formalism discussed in the previous section. Atomic data have been calculated using the  $1/Z$  perturbation theory and approximation for atomic structure

calculations implemented in the MZ code [11, 12]; auto-ionization energies  $E_a$  have been determined using the data from [13]. Our atomic data agree well with the B-like data of Chen and Crasemann [14, 15]. As seen from table 1, to produce B-like Fe dielectronic satellite lines, the energy of the beam has to be in the range from 4.767 keV to 4.809 keV. There are seven lines listed combined into three peaks, which correspond to spectral features that can be identified in the present experimental spectra. For comparison, the lines in table 1 are also labelled according to the notation of [16] where they were discussed in terms of their contribution to Tokamak spectra. Peak 3 is formed by a single, unpolarized line. The other two peaks consist of more than one line that have different degrees of polarization. Relativistic effects are important for the B-like Fe ion, but only one intercombination line (line 7) is observed. In general, the lines contributing to the same peak have different magnitudes and signs of the degree of polarization  $P_0$ . According to equation (1), if the sign of  $P_0$  is positive, the line is predominantly polarized parallel to the electron beam axis, and if the sign of  $P_0$  is negative, the line is predominantly polarized perpendicular to the electron beam axis.

Since we are assuming that the ground state  $1s^2 2s^2 {}^1S_0$  of Be-like ions dominates the electron capture process, then in the pure  $LS$  coupling scheme auto-ionization levels associated with the configuration  $1s2s^2 2p^2$  and terms S and D can be populated, i.e.,

$$1s^2 2s^2 {}^1S_0 + \kappa s \rightarrow 1s2s^2 2p^2 \quad (\text{s-channel}) \quad (6)$$

$$1s^2 2s^2 {}^1S_0 + \kappa d \rightarrow 1s2s^2 2p^2 \quad (\text{d-channel}) \quad (7)$$

where  $\kappa$  characterizes the energy of the electron beam. The corresponding transitions arising from these levels are lines 1, 3, 5, and 6 in table 1. All lines arising from terms populated via the s-channel are unpolarized (see equations (4) and (5)). Hence, line 1 is unpolarized. However, lines arising from terms populated via the d-channel show nonzero degrees of polarization (lines 3, 5, and 6). All other lines, i.e., 2, 4, and 7, occur from levels associated with  $P$  terms, which, due to relativistic effects, are produced by mixing with S and D terms having the same  $J_a$ . The mixing of terms S, D, and P within a complex described by the same parity and the same  $J_a$  increases with  $Z$  and becomes significant for the case of Fe ( $Z = 26$ ). All lines arising from levels with  $J_a = \frac{1}{2}$  are unpolarized. Thus, lines 1 and 4 are unpolarized. Lines arising from levels with  $J_a \neq \frac{1}{2}$  may show polarization. For  $J_a = \frac{3}{2}$ , the levels  ${}^2P$ ,  ${}^2D$ , and  ${}^4P$  are mixed. For  $J_a = \frac{5}{2}$ , the levels  ${}^2D$  and  ${}^4P$  are mixed.

To calculate the polarization of lines arising from P terms, we selected the main term (S or D) depending on which one makes the largest contribution to the level. This main term is then used to calculate the polarization of lines arising from P levels according to equations (4) and (5). For  $J_a = \frac{3}{2}$  and  $\frac{5}{2}$  the main term is  ${}^2D$ . Moreover, levels with  $J_a = \frac{1}{2}$  can be prepared only through the s-channel, while levels with  $J_a = \frac{3}{2}$  and  $\frac{5}{2}$  can be prepared only through the d-channel. This differs from the case of Be-like ions, where we have two and even three S or D terms contributing to each P term, which can be prepared through both channels. Here, for B-like Fe, we have only one main term for each P level. The main term of the upper level of line 2 is  ${}^2D_{3/2}$ , which is the same as for the upper level of line 6, and their lower levels are the same. Thus, line 2 has the same polarization as line 6. Line 7 has the same polarization as line 5. In this case, the main term of the upper level of line 7 is  ${}^2D_{5/2}$ , which is the same as for the upper level of line 5, and their lower levels are the same.

It should be noted that equations (4) and (5) are written for the case of pure  $LS$  coupling. However, they can still be used with confidence in our case. First, we have only two channels of electron capture, which allowed us to treat the upper levels according to the way in which they were prepared. Thus, we can calculate the polarization of lines arising from S or D levels. Second, in all cases we have only one main term for each P level; this allowed us to use the quantum numbers of the main term for the calculation of the polarization of lines arising from

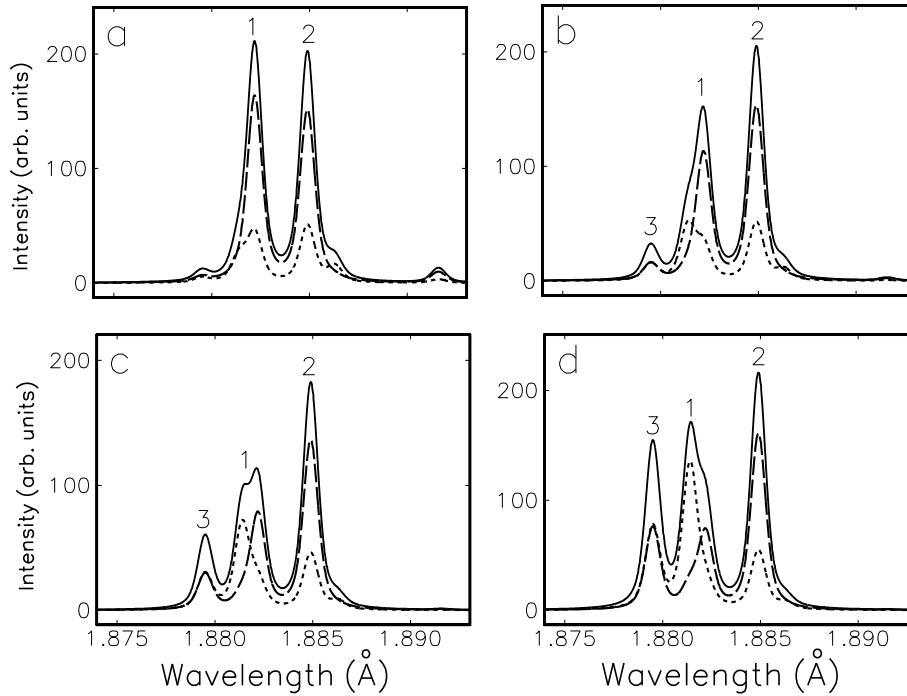


**Figure 1.** Theoretical polarization-dependent spectrum of B-like Fe calculated for four different energies of the electron beam: (a)  $E_b = 4.770$  keV, (b)  $E_b = 4.800$  keV, (c)  $E_b = 4.820$  keV, (d)  $E_b = 4.840$  keV. (---): intensity associated with parallel polarization state, (.....): intensity associated with perpendicular polarization state, (—): total intensity. Spectral features are labelled according to the notation of table 1.

P levels. Third, these results agree well with the values of polarization degrees calculated in j-j coupling in the non-relativistic approximation [17].

### 2.3. Polarization-dependent spectra

Theoretical results for polarization-dependent spectra of dielectronic satellite lines in B-like Fe are presented in figures 1(a)–(d), and figures 2(a)–(c). In figure 1, spectra are displayed for four different energies of the electron beam: (a)  $E_b = 4.770$  keV, (b)  $E_b = 4.800$  keV, (c)  $E_b = 4.820$  keV, and (d)  $E_b = 4.840$  keV. In figure 2, spectra are shown for three different energies of the electron beam: (a)  $E_b = 4.780$  keV, (b)  $E_b = 4.792$  keV, and (c)  $E_b = 4.828$  keV; these three energies were selected to illustrate the details of the theoretical spectra used to interpret the experimental spectra in figures 3–5. All these energies are in the range of the auto-ionization energies listed in table 1. Since we compare synthetic polarization-dependent spectra with experimental spectra recorded at the Livermore EBIT (see section 3), theoretical results were calculated assuming electron beam characteristics, and line profiles suitable for the experimental conditions and instruments used at that facility. The distribution of energies in the electron beam was modelled with a Gaussian function of 47 eV FWHM. Lineshapes were experimentally determined, approximated by numerical fits and used to model line transitions. In particular, for the results presented here we used Voigt lineshapes of Voigt parameter  $a = 0.7$  and FWHM = 0.5 mÅ. The spectral features (peaks) are labelled according to the notation used in table 1.

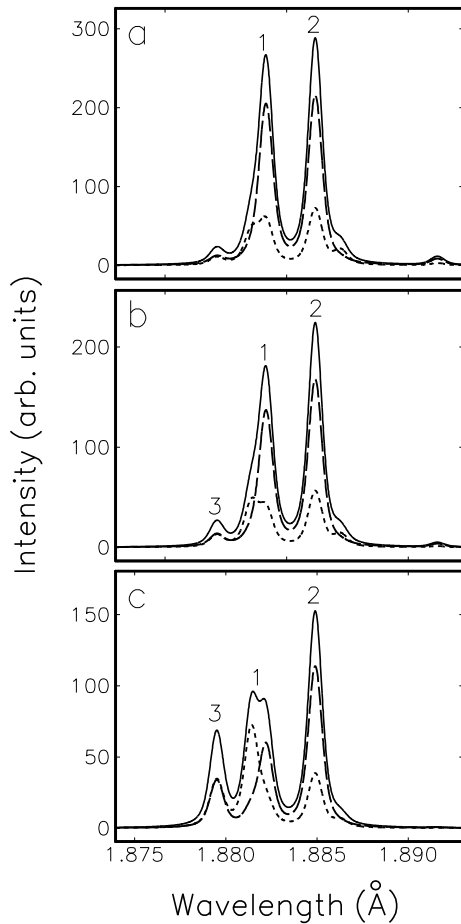


**Figure 2.** Theoretical polarization-dependent spectrum of B-like Fe calculated for three different energies of the electron beam: (a)  $E_b = 4.780$  keV, (b)  $E_b = 4.792$  keV, (c)  $E_b = 4.828$  keV. (---): intensity associated with parallel polarization state, (.....): intensity associated with perpendicular polarization state, (—): total intensity. Spectral features are labelled according to the notation of table 1.

The spectra displayed in figures 1 and 2 illustrate the main properties of the theoretical results: (1) the dependence of the spectra on the electron beam energy  $E_b$ , and (2) the polarization properties of the spectra. First, as the value of the electron beam energy  $E_b$  increases, different electron capture resonances are excited, and the spectrum changes significantly. For  $E_b = 4.770$  keV (the lowest value considered here), two peaks, 1 and 2, are intense. The intensity of peak 1 is a little larger than the intensity of peak 2. Both peaks are predominantly positively polarized, i.e. parallel to the electron beam. Peak 1 consists of three lines, of which lines 2 and 3 are the strongest and have different values of  $E_a$  and polarization. Line 2 has  $E_a = 4.802$  keV and is negatively polarized, i.e. perpendicular to the electron beam, while line 3 has  $E_a = 4.785$  keV and is positively polarized. Line 4 is weak and unpolarized. Thus, for  $E_b = 4.770$  keV, only line 3 contributes significantly to peak 1, and peak 1 is positively polarized. Peak 2 consists of two lines, lines 5 and 6, of which line 5 is the stronger and dominates this peak at all energies. Line 5 is positively polarized, and hence peak 2 is positively polarized at all energies considered. As  $E_b$  increases, the relative intensities of these two peaks, peaks 1 and 2, change. For  $E_b \geq 4.780$  keV peak 2 is more intense than peak 1. Moreover, since peak 3 consists of one unpolarized line (line 1), it is unpolarized at all energies. Peak 2 shows the same positive polarization, but peak 1 starts to show negative polarization on its short-wavelength side. This is caused by the rise of the negatively polarized

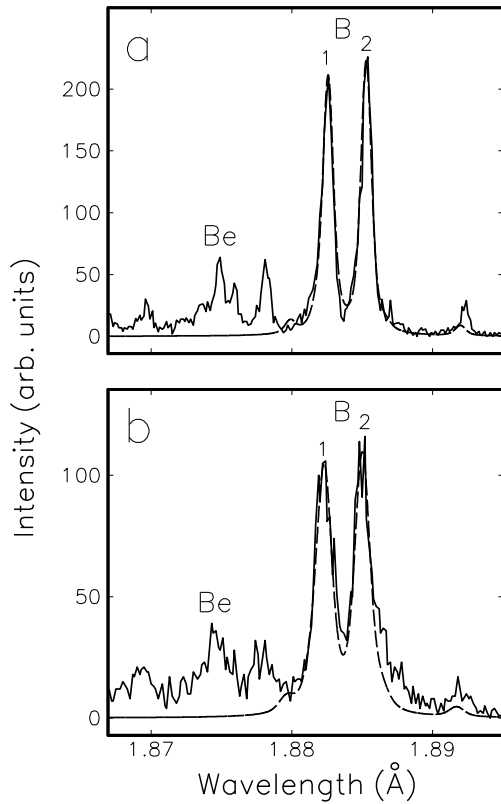


**Figure 3.** Comparison of experimental spectrum (—) and theoretical spectrum of B-like Fe (---) calculated at the electron beam energy  $E_b = 4.780$  keV associated with: (a) almost pure, parallel polarization state, (b) mixture of polarization states. The Be-like spectral features were studied in [10].

line 2. As the energy of the beam continues to increase, the relative contribution of line 2 increases, and the shape of peak 1 changes. As a result, for  $E_b = 4.840$  keV (the highest value considered here) peak 1 is predominantly negatively polarized, peak 2 continues to be positively polarized, and peak 3 is unpolarized.

Three traces are shown in figures 1 and 2 which represent the intensity distributions associated with the parallel polarization state, perpendicular polarization state, and their sum, i.e. the total intensity observed at  $90^\circ$ , calculated according to equations (2) and (3). This way of presenting the results clearly shows the relative contributions of parallel and perpendicular polarization states to the total intensity distribution, and it highlights those peaks (i.e. spectral features) which have significant polarization. The larger the difference between the intensity distributions associated with parallel and perpendicular polarization states, the larger the polarization of the peak. Peaks, where the two traces are identical, are unpolarized. Also, it is interesting to note the differences in relative intensity distributions associated with each polarization-dependent spectrum. This can be illustrated by considering peak 1 whose polarization changes considerably as the energy of the beam increases. The fact that the spectral intensity distributions for the parallel and perpendicular components are different is important, and it can be used to develop polarization spectroscopy diagnostics of electron beams.

### 3. Experimental details and measurements

The experimental spectra were collected at the Lawrence Livermore National Laboratory (LLNL) EBIT. The operation of EBIT has been described in detail in previous articles and

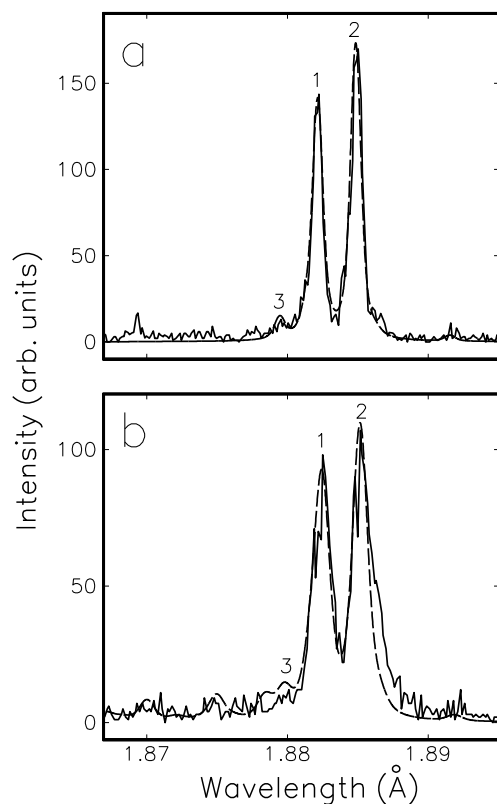


**Figure 4.** Comparison of experimental spectrum (—) and theoretical spectrum of B-like Fe (---) calculated at the electron beam energy  $E_b = 4.792$  keV associated with: (a) almost pure, parallel polarization state, (b) mixture of polarization states.

**Table 2.** The characteristics of the crystals used in the spectral measurements.

	LiF(220)	LiF(200)
Resolving power ( $\lambda/\Delta\lambda$ )	2200	1500
Spacing (2D)	2.848 Å	4.027 Å
Bragg angle	41°	27.5°
Relative reflectivity ( $R_{\perp}/R_{\parallel}$ )	0.12	0.56

reviews [6, 18]. Details of the experimental set-up employed to observe the polarization sensitive spectra can be found in the literature [7–10]. Only the pertinent details specific to this work will be discussed here.

Spectra were accumulated for three electron beam energies, 4.780 keV, 4.792 keV and 4.828 keV. The electron beam energies quoted were calibrated to account for space charge effects [18]. The electron beam energy width (47 eV) was determined experimentally by sweeping over an isolated dielectronic resonance, as described in [19]. At each of the three energies, spectra were accumulated simultaneously by two von Hamos-type crystal spectrometers. The characteristics of the LiF(220) and LiF(200) crystals used in the spectrometers have been discussed previously [10, 20], and are listed in table 2. Here, the  $R_{\perp}$  and  $R_{\parallel}$  are the integrated reflectivities for photons polarized perpendicular and parallel, respectively, to the electron beam axis. These also relate to orientations parallel and perpendicular, respectively, to the spectrometers-dispersion planes. The different relative reflectivities of the crystals provided the experimental polarization sensitivity. The intensity

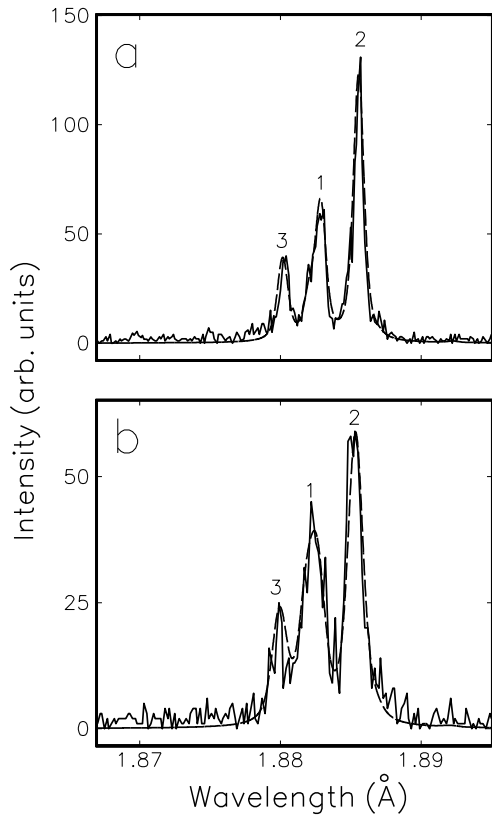


**Figure 5.** Comparison of experimental spectrum (—) and theoretical spectrum of B-like Fe (---) calculated at the electron beam energy  $E_b = 4.828$  keV associated with: (a) almost pure, parallel polarization state, (b) mixture of polarization states.

observed by each spectrometer is given by

$$I_{obs} = R_{\parallel} I_{\parallel} + R_{\perp} I_{\perp}. \quad (8)$$

Since  $R_{\perp}/R_{\parallel}=0.12$  for the LiF(220) crystal, the parallel polarization component is strongly favoured over the perpendicular component, and a nearly pure parallel polarization state is observed. By contrast, the LiF(200) crystal observes a spectrum comprised of a more even mix of polarization states.

#### 4. Comparison of theoretical and experimental results

Figures 3–5 show the comparison between theoretical and experimental spectra. The three electron beam energies indicated, i.e. 4.780 keV, 4.792 keV, and 4.828 keV, corresponding to the energies used to model the experimental data. The top panel shows the spectrum obtained with the LiF(220) crystal, representing emission from an almost pure parallel polarization state. The bottom panel shows the spectrum obtained with the LiF(200) crystal, representing emission from a mixture of both polarization states. As the electron beam energy increases, the observed spectra change significantly. The energy range was chosen to include maximum emission from B-like Fe. As the value of  $E_b$  increases, different electron capture resonances can be excited and the spectral line emission changes. At the lowest energy, there are some features due to Be-like ions but they are smaller in comparison with lines from the B-like ion (figure 3). To aid the comparison, the individual line profiles were modelled using a single Voigt profile (Voigt parameter  $a = 0.7$  and FWHM =  $0.5 \text{ m}\text{\AA}$ ) for the data recorded with

the LiF(220) crystal, and a double Voigt profile (both with parameters  $a = 0.7$  and  $\text{FWHM} = 0.832 \text{ m}\text{\AA}$  but with a relative offset of  $0.2 \text{ m}\text{\AA}$ ) for the LiF(200) crystal data. The values of the electron beam energies used for computing the theoretical spectra were selected to produce the best agreement with the measurements. The values used were never more than  $\pm 4 \text{ eV}$  from the experimental value. This was justified considering comparable uncertainties in the experimental electron beam energy and in the magnitude of the calculated resonance energies. The value of the electron beam  $E_b = 4.780 \text{ keV}$  selected to describe B-like spectral features of the experimental spectra in figures 3(a) and (b) is larger than the value of the electron beam  $E_b = 4.775 \text{ keV}$  selected to describe Be-like spectral features of the same experimental spectra shown in figures 8(a) and (b) from [10]. The disagreement of  $5 \text{ eV}$  can be explained by the fact that the most prominent features in these experimental spectra are B-like ones. They are approximately three times as intense as the Be-like spectral features. The accuracy of the determination of the electron beam energy is obviously higher for more intense spectral lines. Thus, the value  $E_b = 4.780 \text{ keV}$  for this spectrum seems to be more accurate than the previously selected value  $E_b = 4.775 \text{ keV}$ .

Overall, the agreement between theoretical and experimental spectra is very good. The agreement includes good reproduction of the energy dependence of the line emission, the line position, the relative line intensities and the polarization-induced differences between the spectra from the two crystal spectrometers. This good agreement demonstrates that modelling of beam-excited, polarization-dependent spectra can be accomplished with confidence. Some disagreements can be noted. The most notable is for line 7 (figure 3). But line 7 is among the two weakest lines.

The development of sensitive polarization diagnostic tools requires good agreement between theoretical predictions and experimental data for lines that are sensitive markers for polarized line emission. These include the pair of features labelled 1 and 2. The polarization sensitivity arises from the fact that these pairs are made up of lines with nearly opposite polarization properties. Peak 2 is comprised of two lines with close values of auto-ionization energies and different signs of polarization; one of these lines (line 5) dominates this peak for all energies of the electron beam. Peak 1 contains three lines of which two are dominant and have different auto-ionization energies and signs of polarization. As we discussed above, peak 1 changes its polarization with the increase of the energy of the beam, while the polarization of peak 2 does not change. From figures 3–5, a clear difference in the observed intensity ratio of peaks 1 and 2 is seen when comparing the LiF(220) and LiF(200) spectra. This behaviour is reproduced very well by our model calculations. The ratio of the two features can be used as a clear marker for polarization.

## 5. Summary and conclusions

We have extended our previous study of polarization properties of dielectronic satellites in Be-like ions to the case of B-like Fe. We have studied theoretically and experimentally the polarization properties of dielectronic satellite lines of B-like Fe ions excited by an electron beam. Using the photon density matrix formalism, we have calculated the degree of polarization of each dielectronic satellite line. Specifically, from a total of seven lines we found that two of them were unpolarized, while the other ones had different degrees of polarization either predominantly parallel or perpendicular to the electron beam axis. Based on the calculated atomic and polarization characteristics of the satellite lines, the measured line profiles, and the use of a Gaussian distribution function for the electron beam, we have computed the line intensity distributions associated with states of polarization parallel and perpendicular to the electron beam axis. With these spectral distributions we have modelled the

polarization properties of complex dielectronic satellite line spectra of B-like Fe ions excited by an electron beam. We have compared our theoretical spectra with experimental spectra collected at the Livermore EBIT using two crystal spectrometers with different polarization sensitivity. One spectrometer recorded an almost-pure polarization state spectrum, while the other one recorded a mixture of both components. The agreement between theoretical and experimental spectra is good at each electron beam energy. This agreement confirms the good reproduction of the energy dependence of line emission and polarization sensitivity of the satellite spectra. Polarization markers of B-like Fe ion lines as a ratio of differently polarized peaks and the existence of an unpolarized peak have been identified, which can be used to infer the presence of electron beams in low-density plasmas. In conclusion, this paper represents a new test of the theoretical capability to model the polarization-dependence of complicated x-ray spectra excited by a low-density electron beam.

### Acknowledgments

This work was supported by NSF OSR-9353227, DOE EPSCOR, and LLNL contract B336460. Work at LLNL was performed under the auspices of DOE under contract No W-7405-ENG-48 and supported in part by the Office of Basic Energy Sciences, Chemical Sciences Division.

### References

- [1] Percival I and Seaton M J 1958 *Phil. Trans. R. Soc. A* **251** 113
- [2] Haug E 1979 *Sol. Phys.* **61** 129
- [3] Haug E 1981 *Sol. Phys.* **71** 77
- [4] Inal M K and Dubau J 1987 *J. Phys. B: At. Mol. Opt. Phys.* **20** 4221
- [5] Vinogradov A V, Urnov A M and Shlyaptseva A S 1992 *Atomic and Ionic Spectra and Elementary Processes in Plasmas* vol 192 ed P N Lebedev (New York: Nova Science) p 92
- [6] Marrs R E, Beiersdorfer P and Schneider D 1994 *Physics Today* **47** 27
- [7] Beiersdorfer P *et al* 1996 *Phys. Rev. A* **53** 3974
- [8] Beiersdorfer P, Crespo López-Urrutia J, Decaux V, Widmann K and Neill P 1997 *Rev. Sci. Instrum.* **68** 1073
- [9] Shlyaptseva A S, Mancini R C, Neill P and Beiersdorfer P 1997 *Rev. Sci. Instrum.* **68** 1095
- [10] Shlyaptseva A S, Mancini R C, Neill P, Beiersdorfer P, Crespo López-Urrutia J and Widmann K 1998 *Phys. Rev. A* **57** 888
- [11] Vainshtein V L and Safronova U I 1978 *At. Data Nucl. Data Tables* **21** 49
- [12] Safronova U I 1989 *Phys. Scr. T* **26** 59
- [13] Safronova U I and Shlyaptseva A S 1996 *Phys. Scr.* **54** 254
- [14] Chen M H and Crasemann B 1987 *Phys. Rev. A* **35** 4579
- [15] Chen M H and Crasemann B 1988 *At. Data Nucl. Data Tables* **38** 381
- [16] Beiersdorfer P, Phillips T W, Jacobs V L, Hill K W, Bitter M, Von Goeler S and Kahn S M 1992 *Astrophys. J.* **409** 846
- [17] Shlyaptseva A S, Golovkin I E and Safronova U I 1996 *J. Quant. Spectrosc. Radiat. Transfer* **56** 157
- [18] Levine M A *et al* 1989 *Nucl. Instrum. Methods B* **43** 431
- [19] Beiersdorfer P, Phillips T W, Wong K L, Marrs R E and Vogel D A 1992 *Phys. Rev. A* **46** 3812
- [20] Henke B L, Gullikson E M and Davis J C 1993 *At. Data Nucl. Data Tables* **54** 181